

Research Article

Synthesis, structural characterization, and antitumor effect of quercetin-loaded chitosan nanoparticles-stabilized pickering emulsion via suppressing the PI3K/AKT/mTOR signaling pathway

Zainab Noreen^a, Mariam Naveed^b, Abida Raza Rao^c, Shahid Masood Shah^d, Imran Shahid^e, Abdullah R Alzahrani^e, Bushra Ijaz^b, Sidra Rehman^{a,*}

^aDepartment of Biosciences, COMSATS University Islamabad (CUI) Park Road, Islamabad, 45550 Pakistan

^bCenter of Excellence in Molecular Biology (CEMB), University of the Punjab, Lahore, Pakistan, West Canal Bank Road, Lahore, 53700, Pakistan

^cUniversity Institute of Biochemistry and Biotechnology (UIBB), PMAS Arid Agriculture University, Murree Road, Rawalpindi, 46000, Pakistan

^dDepartment of Biotechnology, COMSATS University Islamabad, University Road, Abbottabad, 22060, Pakistan

^eDepartment of Pharmacology and Toxicology, Umm Al-Qura University, AlAbidiyah, P.O. Box 13578, Makkah, Saudi Arabia

ARTICLE INFO

Keywords:

Anticancer activity
Nanoparticles
PI3K/AKT/mTOR signaling pathway
Pickering emulsions
Quercetin
Wound healing

ABSTRACT

Quercetin, a major polyphenolic flavonoid phytoconstituent, exhibits diverse pharmacological activities, including antiviral, antimicrobial, anticancer, and anti-inflammatory effects, and is used in the treatment of metabolic and allergic disorders. However, its pharmaceutical applications are limited by instability, poor aqueous solubility, low permeability, and reduced oral bioavailability. The primary objective of the present study was to overcome these limitations by enhancing the bioavailability and permeability of quercetin by synthesizing Pickering emulsions (PEs) against hepatocellular carcinoma. PEs were prepared by emulsifying an aqueous nanoparticle phase with an oil phase containing quercetin. Quercetin-loaded (CSNPs-QPE) and unloaded (CSNPs-UPE) Pickering emulsions with average particle sizes of ≤ 240 nm and monodisperse characteristics were successfully fabricated. The PEs were characterized using UV-Vis spectrophotometry, particle imaging (Cell Imager EVOS FL), dynamic light scattering (DLS), Fourier-transform infrared spectroscopy (FTIR), and scanning electron microscopy (SEM). The encapsulation efficiency (EE) of the quercetin-loaded PE was 88.8%. *In vitro* release kinetics demonstrated a sustained release of quercetin from CSNPs-QPE, particularly at pH 4.0. Cytotoxicity assays revealed significant cancer cell-killing activity of CSNPs-QPE, comparable to the standard drug doxorubicin, in HepG2 liver cancer cells. Furthermore, CSNPs-QPE promoted apoptosis by inhibiting the PI3K/AKT/mTOR signaling pathway in liver cancer cells with lower IC_{50} ($< \sim 4.5$ $\mu\text{g/mL}$) values as compared to doxorubicin ($> \sim 4$ $\mu\text{g/mL}$). Taken together, our findings support the potential of quercetin-loaded chitosan Pickering emulsions as controlled drug-delivery carriers for suppressing liver cancer cell growth.

1. Introduction

GLOBOCAN 2020 estimated a global cancer incidence of 19.3 million new cases and 10 million deaths in 2020, becoming one of the major factors of mortality worldwide (Sung *et al.*, 2021). In many countries, the increasing incidence of cancer as a predominant cause of death partly reflects a significant decline in mortality from coronary heart disease and stroke relative to cancer (Bray *et al.*, 2021). The rapid rise in both cancer incidence and mortality is largely attributed to population aging and growth, along with changes in the prevalence, frequency, and patterns of cancer-related risk factors, many of which are closely linked with socioeconomic development (Gersten *et al.*, 2002).

Chemotherapy remains one of the most effective cancer treatments; however, cytotoxic agents indiscriminately target rapidly dividing cells,

thereby damaging normal proliferative tissues such as gastrointestinal epithelium, hair follicles, and bone marrow (Ben-Arye *et al.*, 2012). This results in the spectrum of adverse effects, including nausea, alopecia, stomatitis, peripheral neuropathy, cardiomyopathy, leukopenia, and even secondary malignancies (Dehelean *et al.*, 2021; Guruvayoorappan *et al.*, 2015; Hashemzaei *et al.*, 2017). Combination chemotherapy has recently emerged as an optimal strategy in clinical trials due to its enhanced target selectivity, synergistic mechanisms, and reduced drug resistance (Wang *et al.*, 2017). Nevertheless, such regimens are also associated with cumulative toxicities, drug-drug interactions, and increased financial and somatic burdens on patients (Mokhtari *et al.*, 2017). These limitations highlight the urgent need to develop and explore alternative selective anticancer therapies.

Ethnopharmacology has long demonstrated significant potential in disease management (Vafadar *et al.*, 2020), and numerous

*Corresponding author:

E-mail address: sidrarehman@comsats.edu.pk (S. Rehman)

Received: 01 July, 2025 Accepted: 16 October, 2025 Epub Ahead of Print: 27 December, 2025 Published: 16 January, 2026

DOI: 10.25259/JKSUS_1112_2025

phytopharmaceutical compounds with potent anticancer properties have been identified (Wang et al., 2016). Epidemiological studies suggest that diets rich in fruits and vegetables may reduce cancer susceptibility. Among bioactive phytoconstituents, quercetin (QCT), a major plant-derived flavonoid, has shown promising anticancer activity across multiple cancer models. Due to its favorable safety profile and multitarget mechanisms, QCT is considered a potential therapeutic phytochemical for cancer treatment. However, its clinical application remains limited owing to poor bioavailability, low aqueous solubility, chemical instability, and limited intestinal permeability (Wang et al., 2016).

To improve the therapeutic efficacy of QCT, various formulation strategies have been developed. Encapsulating lipophilic quercetin in emulsion-based delivery systems has proven effective in enhancing its pharmacological activity. Nanoencapsulation, which involves entrapping a compound within wall materials at the nanometer scale, can remodel the physicochemical and biological properties of the encapsulated material by increasing surface area and altering particle characteristics (Aranaz et al., 2021; Kyriakides et al., 2021). Pickering emulsions represent an ideal colloidal system for fabricating and delivering anticancer drugs in nanoparticle form (Cardial et al., 2019).

Medium-chain triglycerides (MCTs) are valuable components for emulsion synthesis (Shah et al., 2016). Coconut oil contains more than 48% MCTs, with lauric acid (C12) comprising 45-53% of its total triglyceride content. Lauric acid is particularly advantageous for Pickering emulsion synthesis owing to its rapid metabolism and excellent biocompatibility (Chen et al., 2021). Following ingestion, lauric acid is predominantly transported to the liver, with minimal entry into the lymphatic system as chylomicrons, thereby reducing the risk of conditions such as atherosclerosis and cardiovascular disease. Its metabolism generates ketone bodies capable of crossing the blood-brain barrier to provide energy to muscle and brain tissues (Furuta et al., 2023).

Chitosan (CS), a natural biopolymer with inherent antimicrobial properties, has been extensively used as a promising drug-delivery vehicle. CS exhibits unique characteristics, including biodegradability and biocompatibility with human tissues, without causing allergic reactions or immune rejection. Chitosan nanoparticles (CSNPs) have demonstrated anticancer potential by enhancing immune function (Virmani et al., 2023). Owing to these versatile properties, CS has gained considerable attention in the pharmaceutical industry.

Accordingly, the present study aimed to fabricate and optimize CSNP-stabilized Pickering emulsions, characterize quercetin-encapsulated Pickering emulsions, and evaluate their anticancer activity as a drug-delivery system for quercetin.

2. Materials and Methods

2.1 Materials

Quercetin (QCT) was purchased from Sigma Aldrich, USA. Chitosan (medium molecular weight) was obtained from SolarBio, China. Acetic acid, sodium hydroxide pellets, sodium tripolyphosphate (TPP), and ethanol were purchased from Roth Industries, Germany. Lauric acid was purchased from Uni Chem Co. Ltd., South Korea.

2.2 Methods

2.2.1 Preparation of polymeric chitosan-tripolyphosphate (CSNPs) nanoparticles

CS-TPP nanoparticles were synthesized using the ionic gelation method (Shah et al., 2016). Briefly, a 3% (w/v) chitosan solution was prepared by dissolving chitosan (molecular weight >150 kDa) in 1% (v/v) acetic acid with constant magnetic stirring at 500 rpm and left overnight at room temperature. The pH of the chitosan solution was adjusted to 4.7-4.8. A 0.1% (w/v) TPP solution was then prepared and added dropwise to the chitosan solution to induce nanoparticle formation. The mixture was stirred continuously at 500 rpm for 120 min at room temperature, lyophilized using a freeze dryer, and stored at 4°C until use.

2.2.2 Formulation of quercetin-loaded pickering emulsions (CSNPs-QPE)

Nanoparticle-stabilized Pickering emulsions were prepared following the method of Shah et al. with minor modifications (Shah et al., 2016). The emulsions consisted of two phases: (1) an aqueous phase containing CSNPs and (2) an oil phase of medium-chain triglycerides (MCT). For the oil phase, 8 mg of quercetin was dispersed in 45 mL of MCT and stirred overnight to maximize dissolution. Undissolved quercetin was removed by centrifugation at 14,000 g for 10 min. The aqueous and oil phases (1:1 ratio) were combined in a glass vial and homogenized using a high-speed rotor-stator homogenizer at 10,000 rpm for approximately 3 min at room temperature (Fig. 1). The resulting emulsions were stored in glass bottles at room temperature for further analysis.

2.2.3 Characterization of quercetin-loaded Pickering emulsions

2.2.3.1 Ultraviolet-spectrophotometer

UV spectra of pure quercetin, CSNPs-QPE, and CSNPs-UPE were recorded in the range of 100-400 nm using a HITACHI U-2900

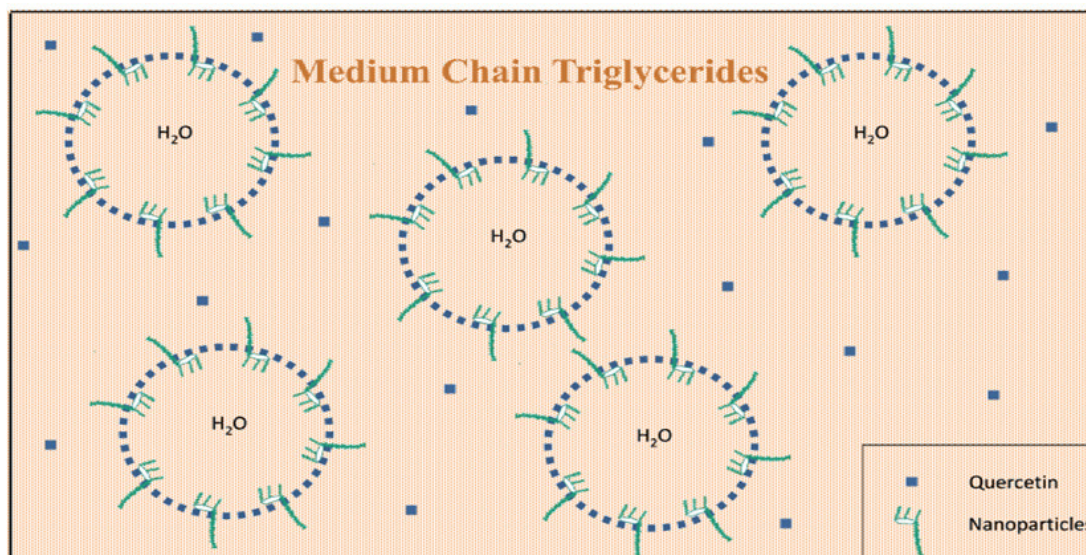


Fig. 1. Schematic representation of the structural organization of CSNPs-QPE.

spectrophotometer (Rehman et al., 2023). Peak shifts were analyzed to confirm emulsion formation and quercetin encapsulation.

2.2.3.2 Microscopic imaging

The morphology of the emulsions was examined using a Cell Imager Invitrogen EVOS FL at 10X, 20X, and 40X magnifications.

2.2.3.3 Quasi-elastic light scattering

The polydispersity index (PDI), emulsion droplet size, and zeta potential of QPE were determined using a Nanotracer Wave-II Zetasizer at 25°C fixing a scattering angle of 90° (Chen et al., 2021). Distilled water served as the dispersing medium. Each sample was analyzed in triplicate, and mean particle sizes were reported.

2.2.3.4 Fourier transform infrared (FTIR) spectroscopy

Fourier Transform Infra-red (FTIR) analysis was done to confirm the synthesis of the emulsion (Chen et al., 2021). The samples were analyzed with an FTIR-8400 spectrophotometer within the wave number range of 400-4000 cm⁻¹.

2.2.3.5 Scanning electron microscopy (SEM)

Scanning electron microscopy was employed for the analysis of surface morphology and particle size of the samples. A small amount of each sample was placed on aluminum stubs, air-dried, coated with gold, and imaged (Chen et al., 2021).

2.2.4 Encapsulation efficiency (EE)

Encapsulation efficiency (indirect method) was determined as described by Jamil et al. (2016) with slight modifications (Jamil et al., 2016). Briefly, freshly prepared CSNPs-QPE samples were centrifuged at 10,000 rpm for 10 min, and the supernatant was carefully collected. The concentration of unencapsulated quercetin in the supernatant was measured spectrophotometrically at 374 nm using a calibrated HITACHI U-2900 UV-Vis spectrophotometer. A quercetin calibration curve (0.63-320 µg/mL) was prepared in the same solvent system and yielded R² = 0.9986. The encapsulation efficiency (%) was calculated as:

$$\text{Percentage EE} = \frac{\text{Quercetin added} - \text{Quercetin encapsulated}}{\text{Quercetin added}} \times 100$$

where Q_{added} is the total quercetin mass introduced into the formulation and Q_{free} is the mass quantified in the supernatant. All measurements were performed in triplicate for each independent batch.

2.2.5 In vitro drug release assay

The release profile of quercetin was evaluated using the dialysis method (Shah et al., 2016). Emulsion samples (5 mL) were sealed in dialysis tubing and immersed in 45 mL phosphate-buffered saline (PBS) at pH 7.4 or 4.0 in 50 mL Falcon tubes. The samples were incubated at 37°C in a shaking incubator set at 120 rpm. At 30-min intervals, 3 mL aliquots of the release medium were withdrawn and replaced with fresh PBS. The drug release was monitored for up to 72 h.

2.2.6 Cell culture

Liver cancer cells (HepG2) were seeded at a density of 3×10⁴ cells in Dulbecco's Modified Eagle Media (DMEM). Fetal Bovine Serum (10%, FBS) was added to DMEM media as a supplement. Streptomycin (100 µg/mL) and penicillin (100 Units/mL) were added to the media. Cells were maintained in 5% CO₂ incubator at 37°C.

2.2.7 Cells passaging

The human liver cancer cell line (HepG2) was cultured in Dulbecco's Modified Eagle Medium (DMEM) supplemented with 1% antibiotics

and 10% FBS. The cells were sub-cultured upon reaching approximately 80% confluency. The used media was aspirated, and 75 cm² culture flasks were washed with phosphate-buffered saline (1X PBS; 5 mL). Trypsin-EDTA (0.5 mL or 1 mL) was added to detach cells, followed by neutralization with fresh medium (3 mL). The cell suspension was centrifuged for 2 min at 3500 rpm. The resulting cell pellet was resuspended in 10 mL of culture medium in culture flasks of 75 cm² and incubated overnight with 5% CO₂ concentration at 37°C in a humidified incubator.

2.2.8 In vitro cytotoxicity (MTT assay)

Cell viability was assessed using the MTT assay with minor modifications (Bahuguna et al., 2017). HepG2 cells were exposed to varying concentrations of CSNPs-QPE, CSNPs-UPE, along with control medium, for 24 h. Subsequently, 10 µL of MTT solution (5 mg/mL in PBS) was added to each well and incubated to allow formation of formazan crystals. Absorbance was measured at 570 nm with a reference wavelength of 620 nm using a BioTek microplate reader. Cell viability (CV%) was calculated as:

$$\text{CV\%} = \frac{\text{Absorbance of sample at 570nm} - \text{Abs of sample at 620nm}}{\text{Absorbance of control at 570nm} - \text{Abs of control at 620nm}} \times 100$$

2.2.9 In vitro migration assay

Cell migration was evaluated using a scratch assay with minor modifications (Rehman et al., 2023). HepG2 cells (5 × 10⁵ cells/well) were seeded into 12-well plates and incubated for 24 h. A cross-shaped scratch was made using a micropipette tip, and wells were washed with PBS. Cells were then treated with CSNPs-UPE, CSNPs-QPE, or doxorubicin (positive control). Wound closure was imaged at 0 and 24 h using a high-resolution inverted microscope.

2.2.10 Genes expression analysis

The gene expression of the PI3K/Akt/mTOR signaling pathway was assessed to evaluate the effects of Pickering emulsions on HepG2 cell proliferation and angiogenesis (Chen et al., 2021). After 48 h of treatment with CSNPs-UPE, CSNPs-QPE, or doxorubicin, total RNA was extracted using TRIZOL® (Life Technologies, Invitrogen). The RNA concentration and quality were measured using an ND-1000 spectrophotometer (Optiplex, USA). First-strand cDNA was synthesized from extracted RNA using M-MLV Reverse Transcriptase (200 U/L; Invitrogen). Quantitative real-time PCR (qRT-PCR) was performed on an ABI 7500 system using SYBR Green Master Mix and sequence-specific primers described previously (Rehman et al., 2025). GAPDH served as the internal housekeeping control. The relative gene expression was calculated using the comparative Ct (2^{-ΔΔCt}) method, normalized to GAPDH expression. All reactions were performed in triplicate to ensure reproducibility.

3. Results

3.1 Synthesis of CSNPs-QPE

CSNPs-QPE were synthesized using the ionic gelation method at a chitosan-to-TPP ratio of 3:1 (Fig. 2). The formation of a white, milky suspension confirmed the interaction between the amine group (+NH₃) of chitosan and the phosphate group (PO₄⁻) of TPP.

3.2 Characterization of CSNPs-QPE

3.2.1 UV-Vis spectroscopy

UV-Visible absorption spectra were recorded to confirm emulsion formation and quercetin encapsulation using a HITACHI U-2900 spectrophotometer. Samples were scanned over the wavelength range of 100 to 400 nm. Pure quercetin exhibited a characteristic absorbance peak at 375 nm, whereas CSNPs-QPE showed distinct peaks at 378.8 nm and 341 nm (Fig. 3a). The observed red shift from 375 nm to 378.8 nm confirmed successful CSNPs-QPE formation. This special red shift

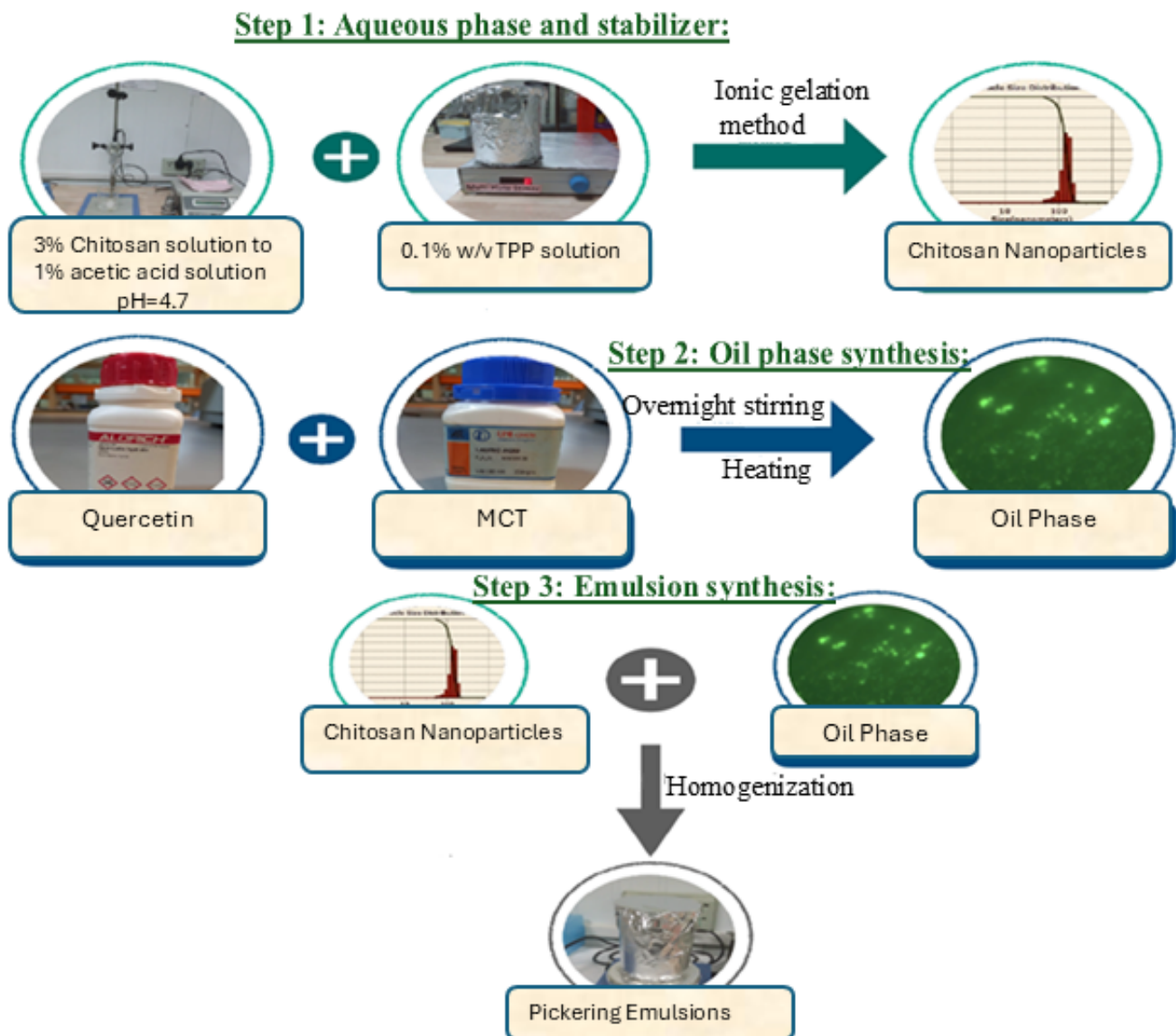


Fig. 2. Schematic illustration of the synthesis process for quercetin-loaded and unloaded Pickering emulsions.

is attributed to microenvironmental changes around the quercetin chromophore, likely resulting from hydrogen-bonding, polarity changes, and π - π stacking within the polymeric matrix. (Fig. 3a). The additional absorbance at ~ 341 nm, along with the disappearance of free-quercetin signals in the supernatant, further supports that quercetin molecules were incorporated into the emulsion droplets rather than remaining freely dissolved in the oil phase. In contrast, the unloaded Pickering emulsions (CSNPs-UPE) exhibited a distinct absorption peak at 287 nm, corresponding to the presence of oil and aqueous phases without quercetin.

3.2.2 Fourier transform infra-red spectroscopy

FTIR analysis was performed to investigate chemical interactions and confirm emulsion synthesis. Moisture-free KBr pellets were used to avoid spectral noise. The FTIR spectra of CSNPs-UPE and CSNPs-QPE have been presented in Fig. 3(b).

- **CS-TPP nanoparticles** showed characteristic peaks at 3332 cm^{-1} and 1640 cm^{-1} . Broad band attributed to O-H stretching (phenolic -OH of quercetin and surface hydroxyls) and N-H stretching from chitosan. A shift of the chitosan peak from 1630 cm^{-1} to 1640 cm^{-1} indicated successful nanoparticle formation. The observed upshift

upon nanoparticle formation ($1630 \rightarrow 1640\text{ cm}^{-1}$) is typical of electrostatic crosslinking with TPP (interaction of $-\text{NH}_3^+$ with PO_4^{3-}), supporting successful ionic gelation (Fig. 3b).

- **Pure lauric acid** exhibited peaks at 2853 cm^{-1} and 2942 cm^{-1} ($-\text{CH}_3$ and $-\text{CH}_2$ stretching), 931 cm^{-1} (hydroxyl wagging), 723 cm^{-1} (C-H bending), 1702 cm^{-1} (carbonyl group), and 1292 cm^{-1} (C-O stretching) (Jiang et al., 2018).
- **Pure quercetin** displayed unique peaks for stretching and aromatic bending between 1095 – 1614 cm^{-1} and phenolic -OH bending between 1213 – 1429 cm^{-1} .
- **CSNPs-UPE** showed peaks at 2879 , 2945 , 916 , 750 , 1707 , and 1286 cm^{-1} . 916 , 750 cm^{-1} peaks are associated with alkyl bending (lauric acid) and out-of-plane aromatic C-H wagging; their preservation in CSNPs-UPE indicates intact oil-phase signatures in the emulsion.
- **CSNPs-QPE** exhibited peaks at 3304 , 1230 , and 1448 cm^{-1} corresponding to phenolic -OH bending, confirming Pickering emulsion formation. The 1230 cm^{-1} band in CSNPs-QPE specifically suggests quercetin's phenolic C-O contribution or new C-O interactions at the particle interface. In CSNPs-QPE, the band at 3304 cm^{-1} is consistent with phenolic OH involvement and often broadens/changes when hydrogen bonding occurs.

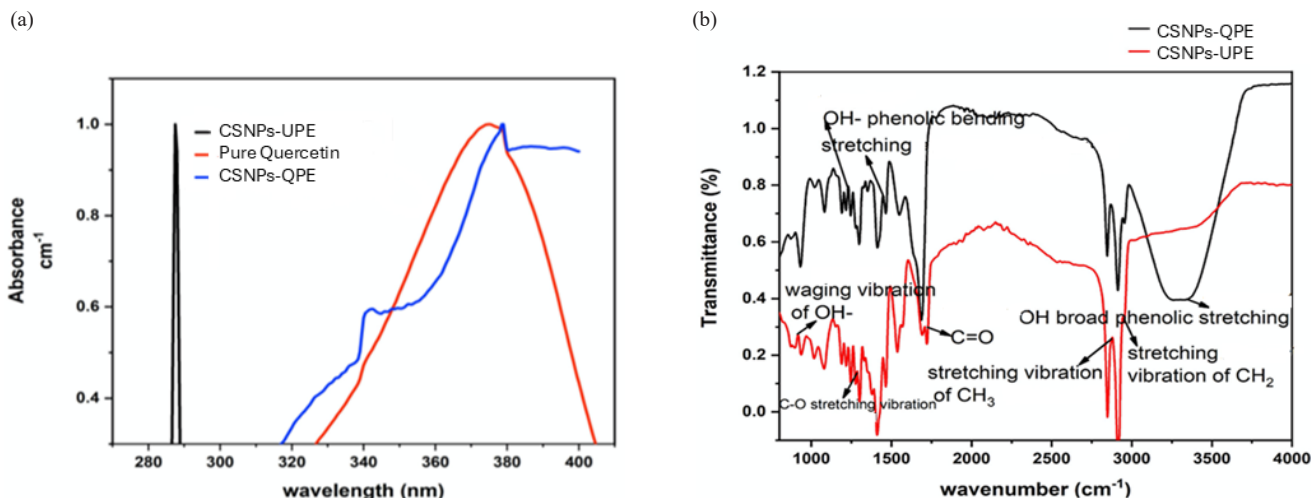


Fig. 3. (a) UV-Visible spectra of CSNPs-QPE, CSNPs-UPE, and pure quercetin. The observed peak shifts from 375 to 379 nm and from 330 to 341 nm indicate bonding interactions among the constituent compounds of CSNPs-QPE and CSNPs-UPE. (b) FTIR spectra of CSNPs-QPE and CSNPs-UPE. CSNPs-QPE: quercetin-loaded chitosan Pickering emulsion; CSNPs-UPE: unloaded chitosan Pickering emulsion.

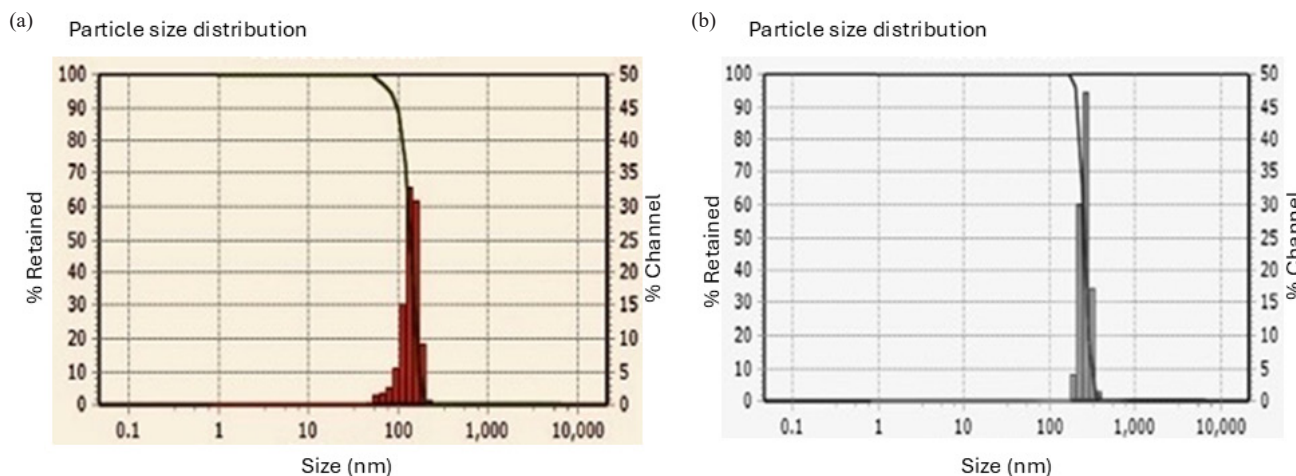


Fig. 4. Measurement of size, PDI, and zeta potential of nano-formulations through DLS. (a) CSNPs nanoparticles, (b) CSNPs-QPE.

3.2.3 Dynamic light scattering (DLS)

The particle size and zeta potential of the formulations were determined using dynamic light scattering (DLS) (Fig. 4). The average particle sizes of CSNPs and CSNPs-QPE were 124 nm and 238 nm, respectively. The corresponding zeta potential values were +44.5 mV for CSNPs and +59.5 mV for CSNPs-QPE, indicating strong electrostatic repulsion and high colloidal stability. Both formulations (CSNPs and CSNPs-QPE) showed narrow particle size distribution with polydispersity indices of 0.1192 and 0.457, respectively (Table 1). The PDI value ≈ 0.46 for quercetin-loaded Pickering emulsions reflects a slight increase in size heterogeneity likely resulting from oil loading and emulsification processes.

Table 1. Characterization of CSNPs and CSNPs-QPE depicting size, zeta potential, PDI, %EE, and % *in vitro* release values.

Samples	Size (nm)	Zeta potential (mV)	PDI	%EE	% Drug Release
CSNPs	124	+ 44.5	0.12	-	-
CSNPs-QPE	238	+ 59.5	0.45	88.5 \pm 2.0 (n=3)	81 (pH 4.0) 67 (pH 7.4)

3.2.4 Optical imaging of CSNPs-QPE

The morphology of the emulsions was examined using a Cell Imager Invitrogen EVOS FL. As shown in Fig. 5, the emulsions appeared spherical and uniform, consistent with DLS results.

3.2.5 Scanning electron microscopy

SEM analysis confirmed the size and surface morphology of CSNPs-QPE. The images revealed uniformly shaped spherical emulsions (Fig. 5), further supporting optical microscopy findings. Further, SEM images showed uniform, spherical particles with smooth surfaces and no obvious large-scale aggregation.

3.2.6 Encapsulation efficiency of CSNP-QPE

Encapsulation efficiency (EE) is a key parameter in nanodrug delivery. Quercetin was efficiently encapsulated within the oil phase of the emulsions, achieving an EE of 88.8% (Table 1). This high EE suggests that CSNPs-QPE can serve as an effective drug delivery system.

3.3 *In vitro* release profile of CSNPs-QPE

The release of quercetin from CSNPs-QPE was evaluated at two pH scales, i.e., pH 4.0 and pH 7.4 to simulate physiological and

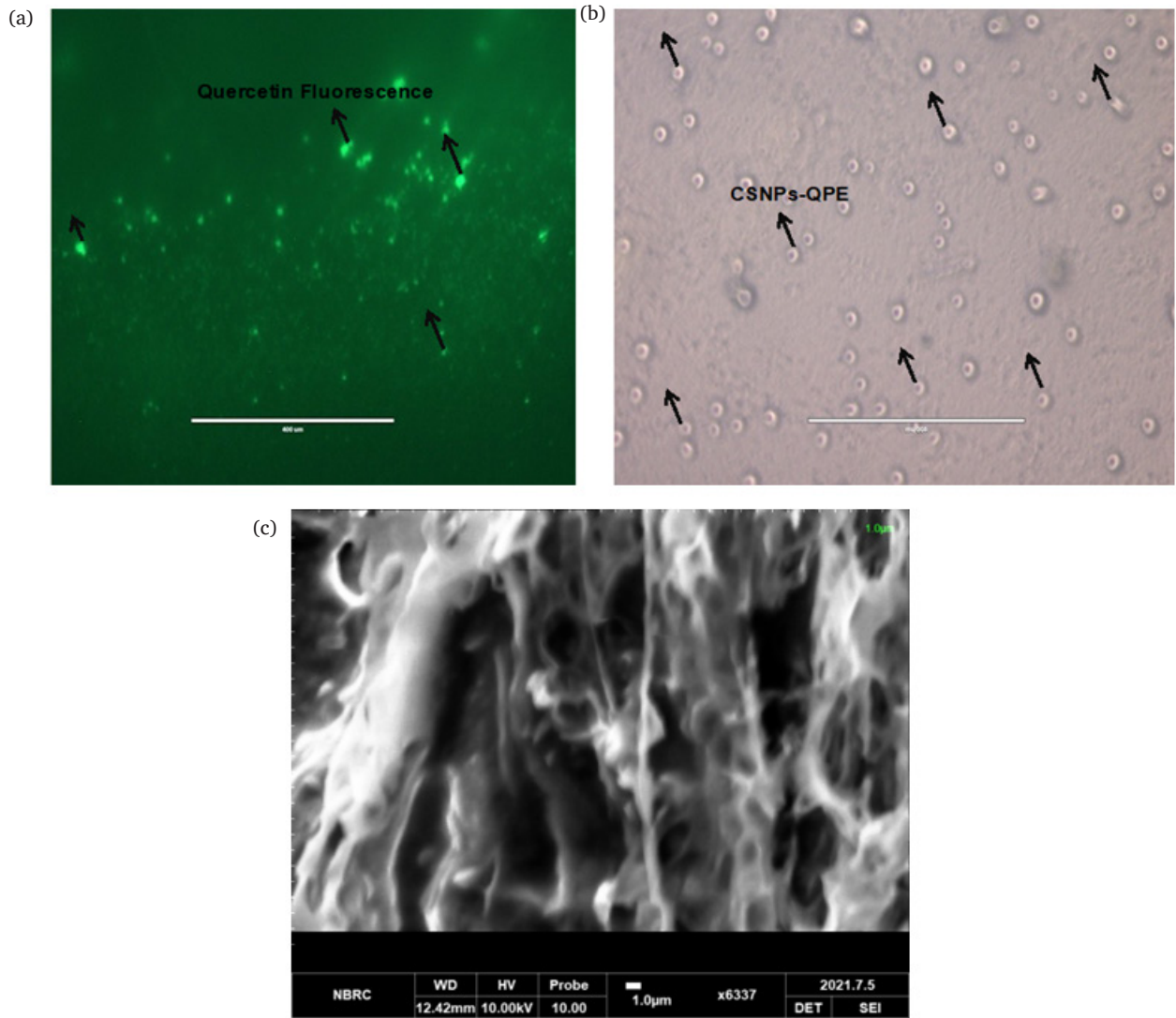


Fig. 5. Nano-formulations viewed on cell imager EVOS at 40X magnification (a) CSNPs-QPE (GFP filter). (b) CSNPs-QPE transmittance filter. (c) Cell morphology visualization using Scanning Electron Microscopy of CSNPs-QPE.

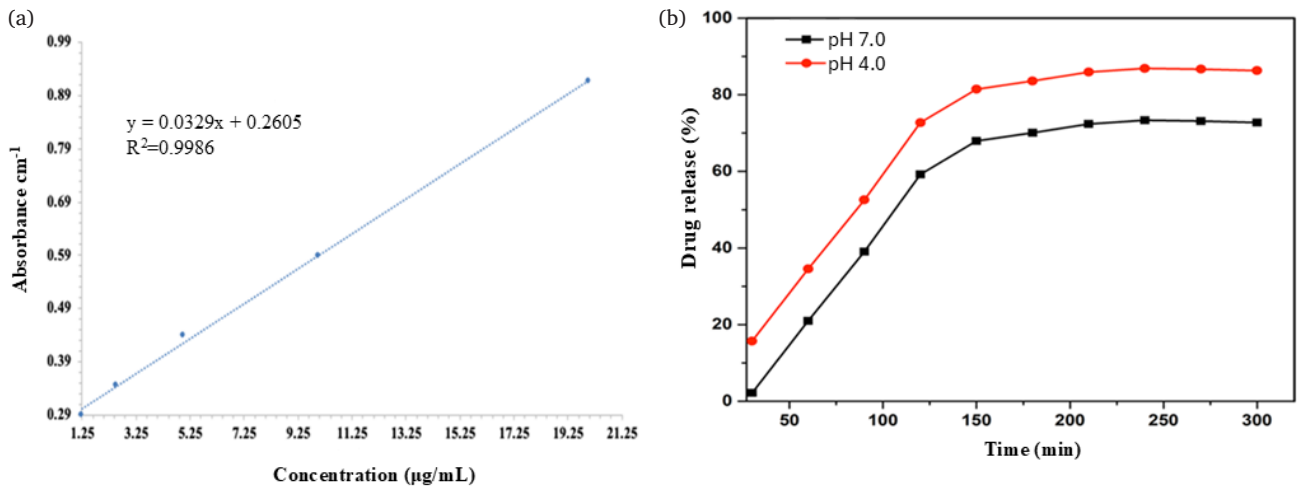


Fig. 6. (a) Encapsulation Efficiency of CSNPs-QPE. Representing the R2 value, quercetin was encapsulated efficiently in the oil phase of the emulsion. The percentage encapsulation efficiency was calculated to be 88.8%. (b) Graphical representation of *in vitro* drug release profile for CSNPs-QPE at pH 7.4 and 4.0. A sustained drug release pattern was observed for CSNPs-QPE.

Table 2. Kinetic modelling of quercetin release profile of encapsulated Pickering emulsions

Samples	Zero order R ²	First order R ²	Korsmeyer-Peppas R ²	Higuchi R ²
CSNPs-QPE (pH4.0)	0.9081	0.9594	0.9534 n=0.20	0.9471
CSNPs-QPE (pH7.4)	0.9428	0.9605	0.9611 n=1.12	0.9563

acidic tumor environments (Fig. 6). After 30 min, drug release was approximately 2% at pH 7.4 and 15% at pH 4.0, indicating initial diffusion resistance due to the emulsion bilayer. After 2.5 h, a marked increase in release, reaching 67% and 81% at pH 7.4 and 4.0, respectively, followed by a slower diffusion phase. Overall, a higher cumulative release at pH 4.0 indicated increased drug diffusion under acidic conditions and a sustained release pattern. Further, release kinetics analysis further revealed that at pH 4.0, the quercetin release from CSNPs-QPE showed a moderate correlation ($R^2 = 0.9081$) with the zero-order model, indicating a nearly constant release rate with slight deviations over time (Table 2). The first-order model exhibited an excellent fit ($R^2 = 0.9594$), demonstrating that the release rate is concentration-dependent. The Higuchi model showed a strong linear relationship ($R^2 = 0.9471$), confirming that Fickian diffusion through the polymeric matrix primarily governs release. The Korsmeyer–Peppas model depicted a strong linear correlation ($R^2 = 0.9531$) with a release exponent (n) of 0.20, indicating that the drug release mechanism follows Fickian diffusion, with the release rate mainly governed by diffusion through the matrix (Table 2).

3.4 Anti-tumour activity

3.4.1 In vitro cytotoxicity in liver cancer cells

The cytotoxic effects of doxorubicin-loaded (CSNPs-QPE) and unloaded (CSNPs-UPE) emulsions were evaluated against HepG2 liver cancer cells using the MTT assay at concentrations ranging from 80 to

2.5 µg/mL. In 96 wells plates, cells with 80-85% confluency were treated with doxorubicin, CSNPs-UPE, and CSNPs-QPE. Cell viability results have been shown in Fig. 7. The IC₅₀ value of CSNPs-QPE was 20 µg/mL after 48 h of formulation exposure (Fig. 7b). At a concentration of 80 µg/mL, CSNPs-QPE inhibited more than 90% of the cell proliferation, comparable to doxorubicin (~94%) (Fig. 7a). CSNPs-QPE exhibited significant dose-dependent inhibition of cancer cell growth, consistent with the sustained drug release profile.

3.4.2 Wound healing assay

Cell migration was assessed using a scratch assay at CSNPs-QPE concentrations of 5 µg/mL and 20 µg/mL. After 24 h, wound closure was 72%, 78%, and 100% for CSNPs-UPE, CSNPs-QPE, and doxorubicin, respectively, at 5 µg/mL (Fig. 8). At 20 µg/mL, wound closure was 69%, 74%, and 100% for CSNPs-UPE, CSNPs-QPE, and doxorubicin, respectively.

3.4.3 Evaluating antitumor effect of CSNPs-QPE upon liver cancer cells through PI3K/Akt/mTOR pathway

The anticancer activity of CSNPs-QPE was further evaluated by analyzing the PI3K/Akt/mTOR signaling pathway in HepG2 cells. Cells were treated with CSNPs-UPE, CSNPs-QPE, or DOX for 48 h. DOX served as a positive control.

- **PI3K Expression:** CSNPs-QPE at 5 µg/mL significantly inhibited PI3K expression compared to the negative control and DOX at the same concentration (Fig. 9). CSNPs-QPE exhibited a lower IC₅₀ value (4.5 µg/mL) than DOX (6.67 µg/mL) for PI3K inhibition (Fig. 10).
- **Akt Expression:** Both DOX and CSNPs-QPE caused significant downregulation of Akt ($p < 0.0001$). At 5 µg/mL, CSNPs-QPE inhibited 81% of Akt expression, whereas DOX inhibited 75% (Fig. 11). The IC₅₀ values for Akt inhibition were 2.24 µg/mL for CSNPs-QPE and 3.43 µg/mL for DOX (Fig. 12).

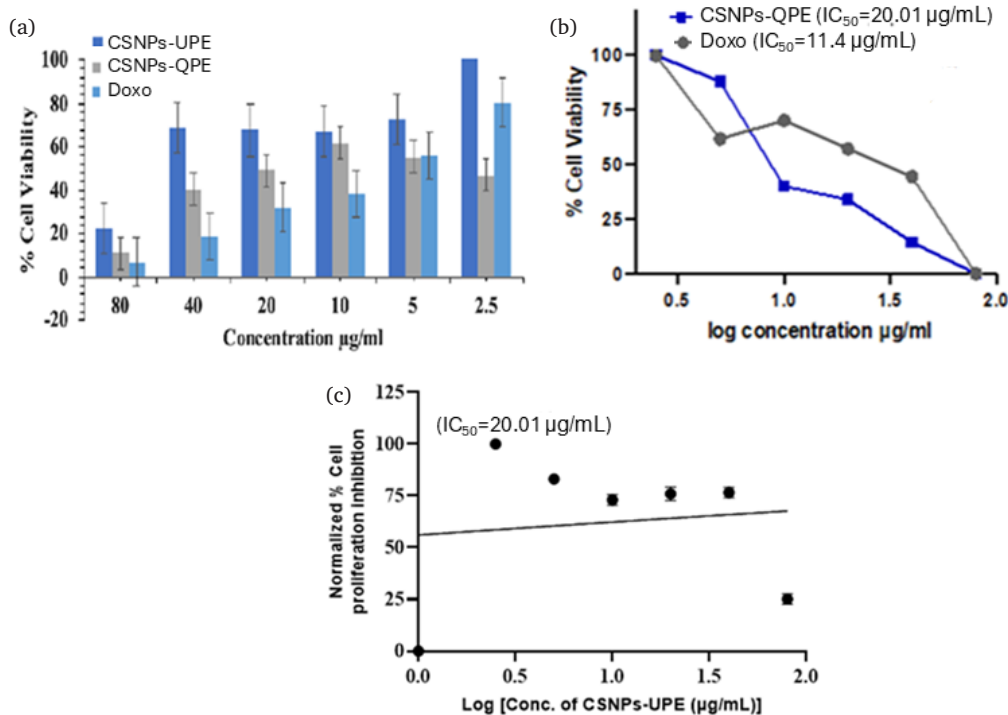


Fig. 7. Percentage cell viability of HepG2 liver cancer cells treated with CSNPs-QPE, CSNPs-UPE, and Doxorubicin (Doxo). Cell viability was assessed following 24 h treatment with varying concentrations of each formulation. The results indicate that both CSNPs-QPE and CSNPs-UPE show reduced inhibitory effects at concentrations below 5 µg/mL, while a pronounced dose-dependent cytotoxicity was observed at higher concentrations. (a) A bar graph representing % cell proliferation of CSNPs-QPE, CSNPs-UPE and doxorubicin. (b) Cell viability profile depicting IC₅₀ for CSNPs-QPE and doxorubicin (c) Cell viability profile depicting IC₅₀ for CSNPs-UPE.

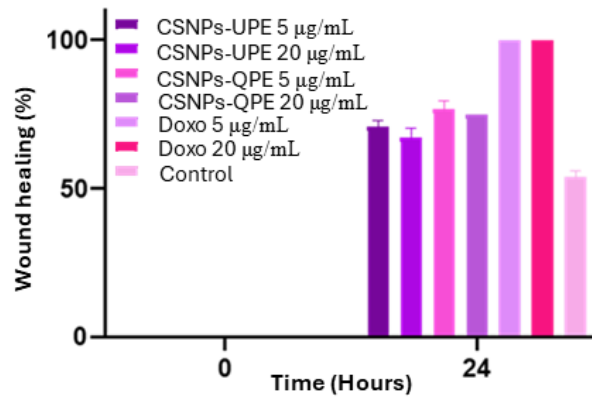


Fig. 8. Analysis of migration assay for CSNPs-UPE, CSNPs-QPE, and Doxo at 5 µg/mL and 20 µg/mL in HepG2 cells.

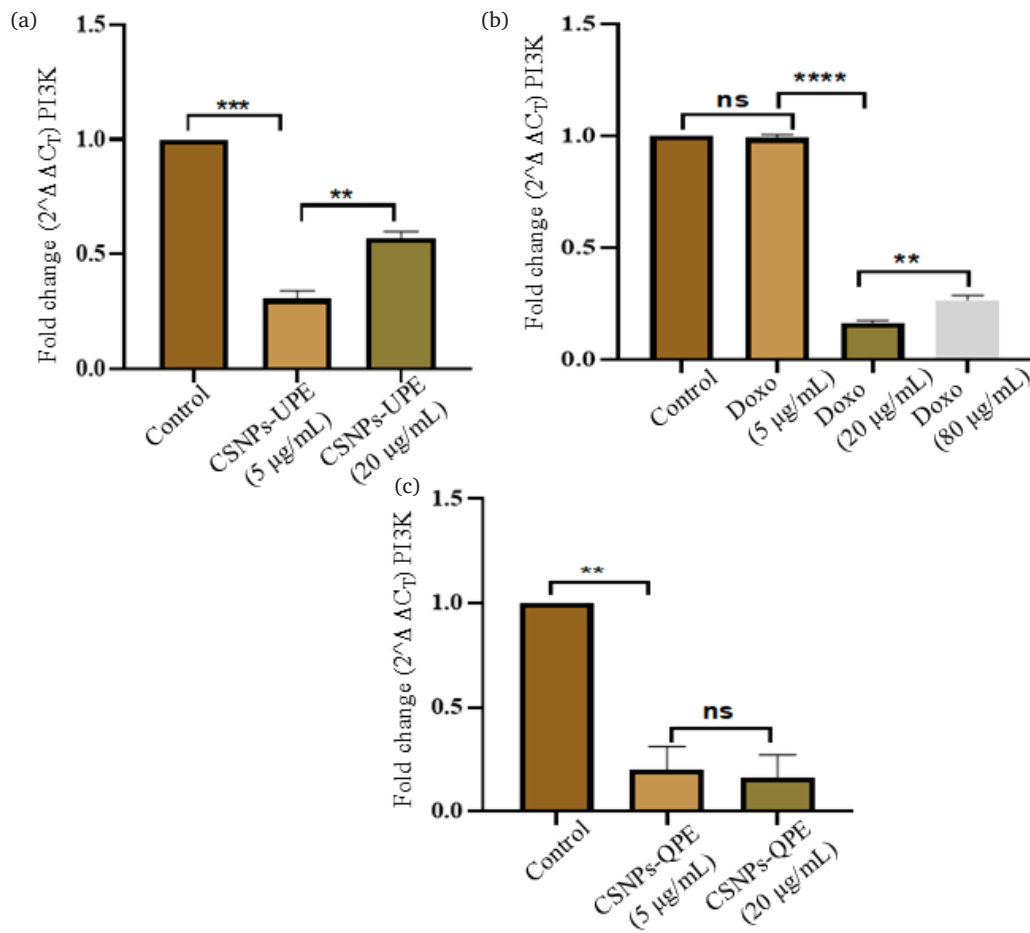


Fig. 9. Quantitative real-time PCR (RT-qPCR) analysis of *PI3K* gene expression in HepG2 cells treated with CSNPs-UPE, doxorubicin (DOX), and CSNPs-QPE. (a) CSNPs-UPE at 5 µg/mL induced a modest reduction of approximately 0.5-fold in *PI3K* expression. (b) DOX at 20 µg/mL resulted in nearly 80% inhibition of *PI3K* mRNA levels. (c) CSNPs-QPE at 5 and 20 µg/mL produced a pronounced downregulation, with up to 0.9-fold reduction in *PI3K* expression, demonstrating potent gene-silencing effects. Data are expressed as mean ± standard deviation (n = 3). Statistical significance: $p < 0.05$, $p < 0.01$, $p < 0.001$ versus control.

- mTOR Expression:** CSNPs-QPE induced marked downregulation of mTOR compared to CSNPs-UPE and DOX (Fig. 13). At 5 µg/mL, CSNPs-QPE inhibited >90% of mTOR expression ($p < 0.0001$), while DOX showed minimal inhibition at the same concentration. At 20 µg/mL, mTOR inhibition reached 90% with CSNPs-QPE and 75% with DOX. The IC_{50} values were 2.24 µg/mL for CSNPs-QPE and 10.01 µg/mL for DOX (Fig. 14).

4. Discussion

Nanodrug delivery systems facilitate the efficient transport of natural products as therapeutic agents. Such systems enhance drug release profiles in a sustained manner, reduce side effects, improve bioactivity, and enable targeted delivery (Islam et al., 2017). Quercetin is a potent bioactive compound present in various functional foods;

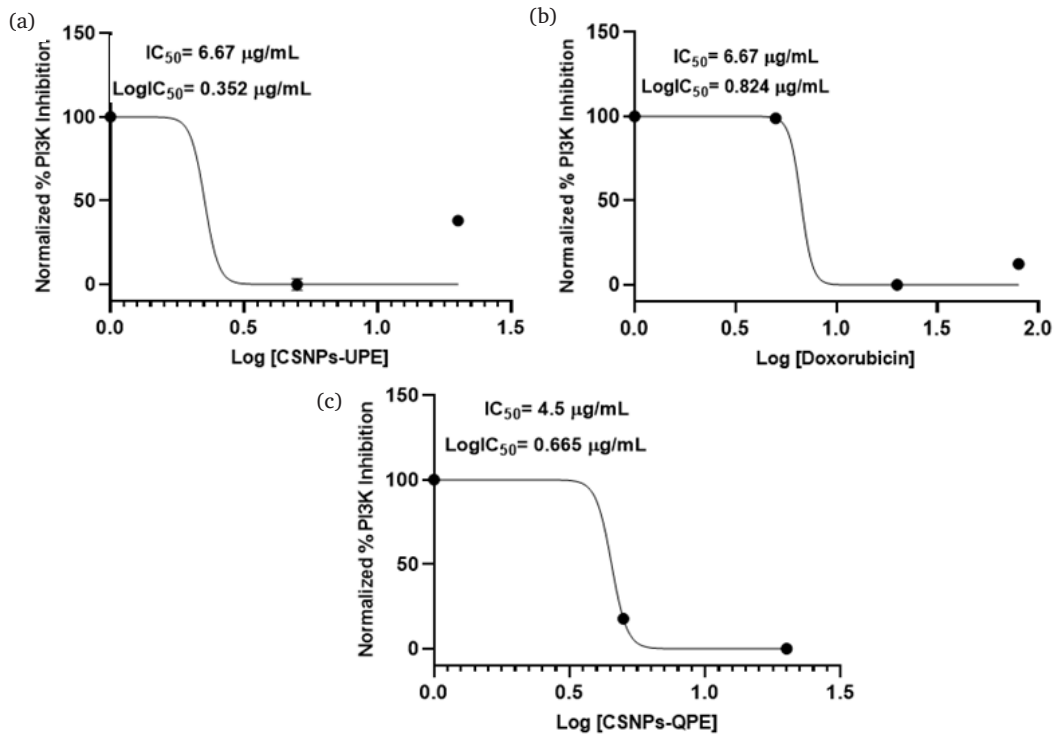


Fig. 10. (a-c) Half-maximal inhibitory concentration (IC_{50}) analysis of HepG2 cells treated with CSNPs-UPE, doxorubicin (DOX), and CSNPs-QPE. Dose–response curves show that CSNPs-QPE achieved a significantly lower IC_{50} value (4.5 $\mu\text{g}/\text{mL}$) compared with the standard chemotherapeutic agent DOX (6.67 $\mu\text{g}/\text{mL}$) and the unloaded formulation CSNPs-UPE, indicating enhanced cytotoxic potency of the quercetin-loaded Pickering emulsion. Data represent mean \pm standard deviation of three independent experiments.

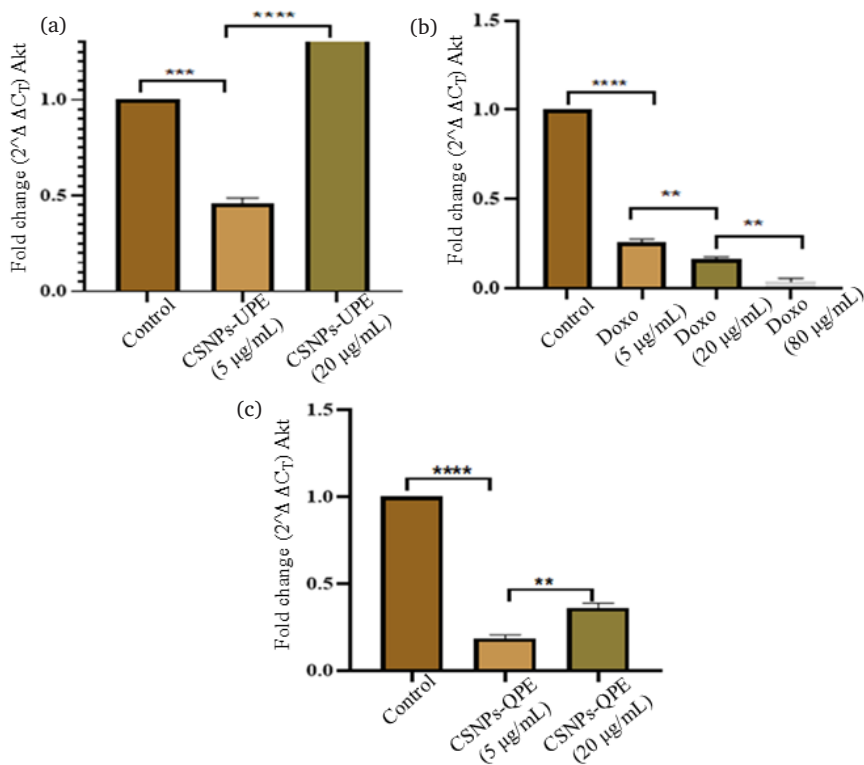


Fig. 11. (a) Real-time PCR analysis revealed no significant fold change in *AKT* gene expression following treatment with CSNPs-UPE at a concentration of 20 $\mu\text{g}/\text{mL}$. (b) In contrast, doxorubicin (DOX) at a high concentration of 80 $\mu\text{g}/\text{mL}$ produced a marked suppression of *Akt* expression, with >90% inhibition relative to the untreated control. (c) Notably, exposure of HepG2 cells to CSNPs-QPE at a low dose (5 $\mu\text{g}/\text{mL}$) resulted in >80% inhibition of *AKT* gene expression, demonstrating potent downregulation at sub-cytotoxic levels. Data are presented as mean \pm standard deviation (SD) from three independent experiments. Statistical significance was determined relative to the control group ($*p < 0.05$, $**p < 0.01$, $***p < 0.001$).

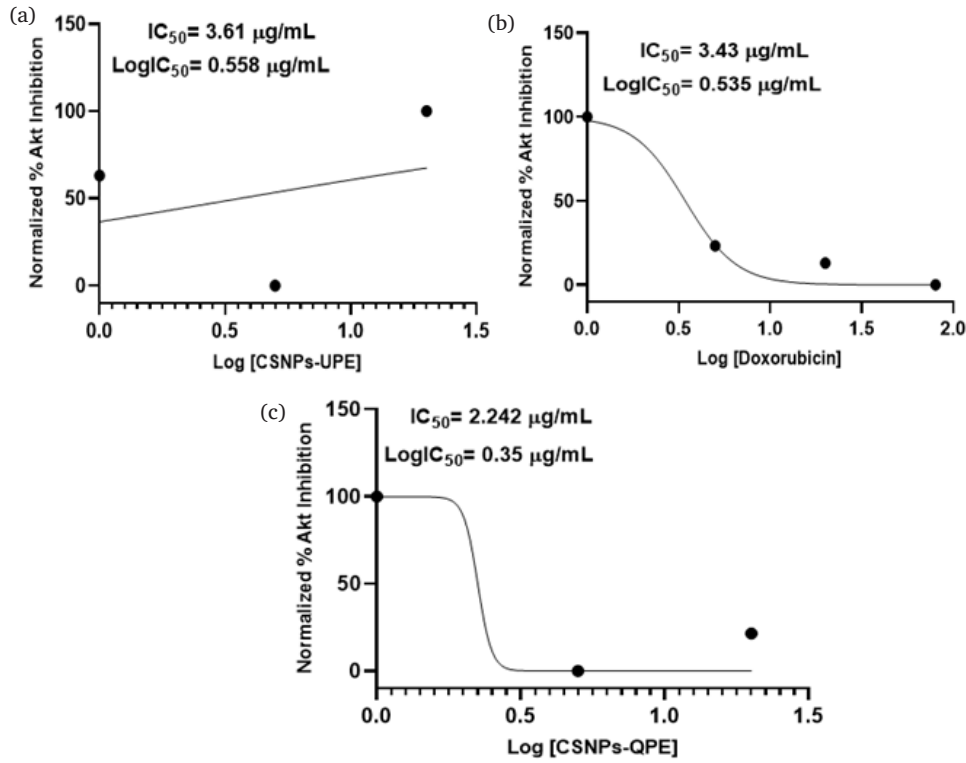


Fig. 12. (a-c) Half-maximal inhibitory concentration (IC_{50}) analysis demonstrated that CSNPs-QPE exhibited a markedly lower IC_{50} value (2.24 $\mu\text{g/mL}$) compared with the standard chemotherapeutic agent doxorubicin (3.43 $\mu\text{g/mL}$) and the unloaded formulation CSNPs-UPE. This finding indicates the superior cytotoxic efficacy of the quercetin-loaded Pickering emulsion relative to both the conventional drug and the unloaded control.

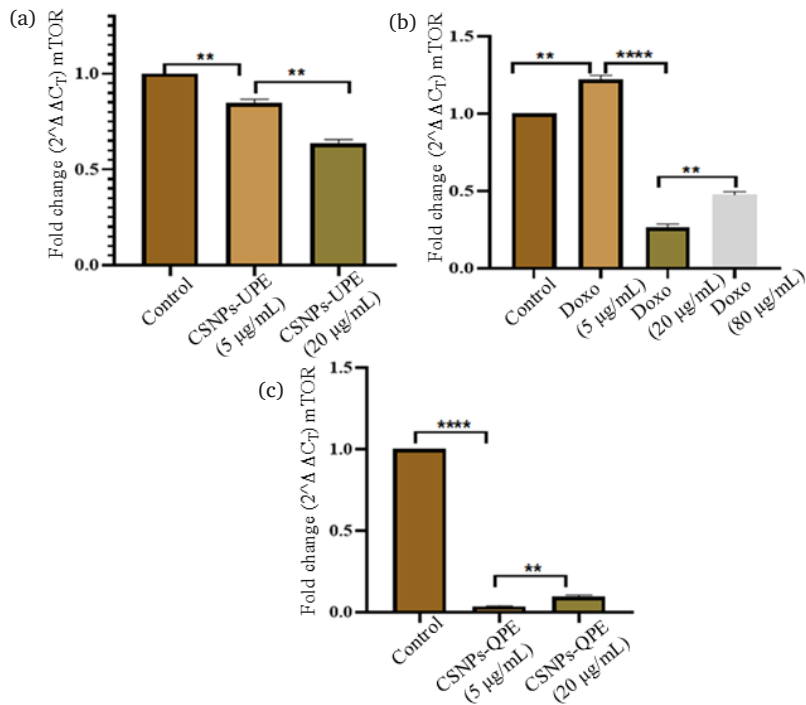


Fig. 13. Quantitative real-time PCR (RT-qPCR) analysis of *mTOR* gene expression in HepG2 cells following treatment with CSNPs-UPE, doxorubicin, and CSNPs-QPE. (a) CSNPs-UPE at 5 $\mu\text{g/mL}$ induced only a 0.2-fold change in *mTOR* expression, indicating minimal inhibitory activity. (b) DOX at 80 $\mu\text{g/mL}$ produced >70% suppression of *mTOR* mRNA levels. (c) CSNPs-QPE at 5 and 20 $\mu\text{g/mL}$ achieved >90% inhibition of *mTOR* expression, demonstrating potent down-regulatory effects. Data are presented as mean \pm standard deviation ($n = 3$). Statistical significance: $p < 0.05$, $p < 0.01$, $p < 0.001$ versus control.

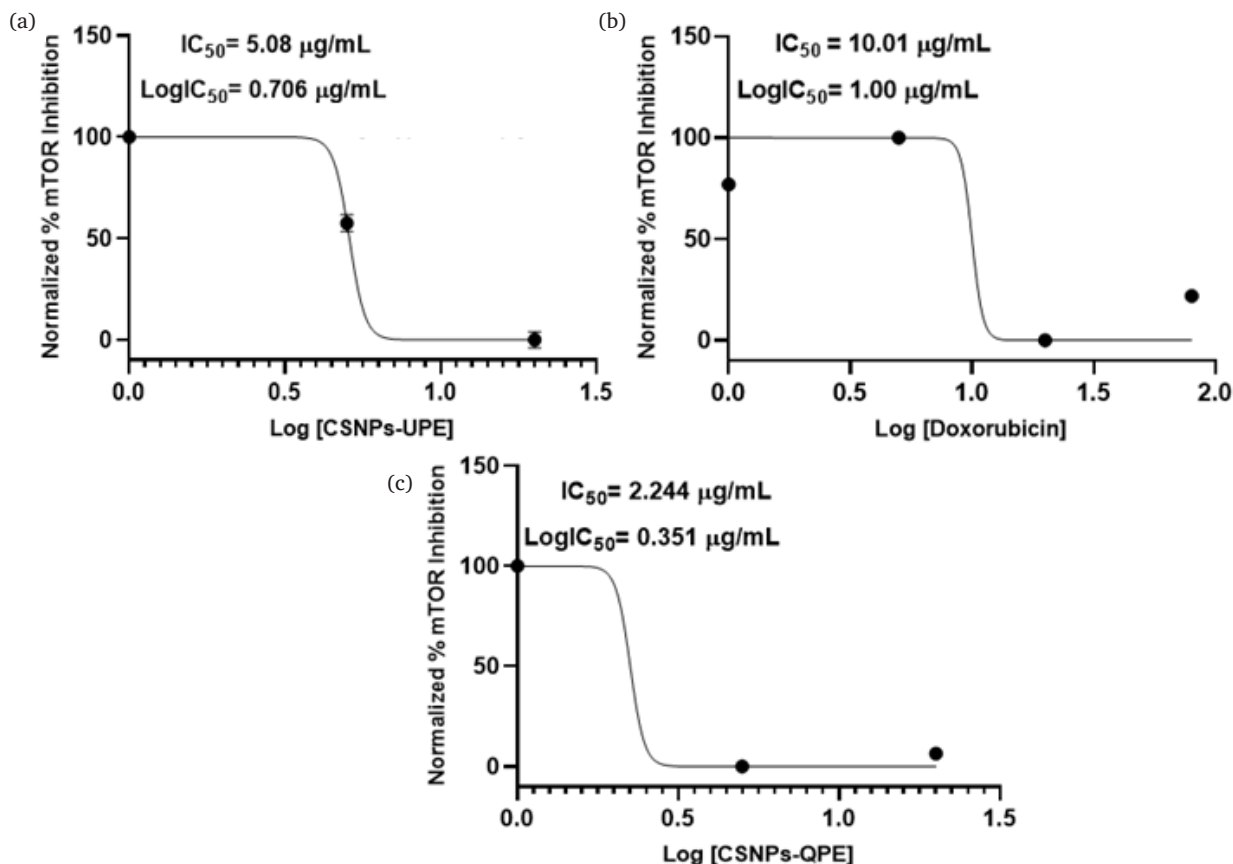


Fig. 14. (a-c) Half-maximal inhibitory concentration (IC_{50}) analysis of HepG2 cells treated with CSNPs-UPE, doxorubicin, and CSNPs-QPE. Dose-response curves demonstrate that CSNPs-QPE achieved a significantly lower IC_{50} value (2.24 $\mu\text{g/mL}$) compared with the standard chemotherapeutic agent DOX (10.01 $\mu\text{g/mL}$) and the unloaded formulation CSNPs-UPE, indicating superior cytotoxic potency of the quercetin-loaded Pickering emulsion. Data represent mean \pm standard deviation of three independent experiments.

however, its therapeutic use is limited due to poor water solubility, low gastrointestinal (GI) membrane permeability, and the need for high doses, which can lead to acute toxicity, kidney dysfunction, gastrointestinal disturbances, and allergic reactions (Andres *et al.*, 2018). Nanoscale formulations of quercetin have been developed to address these limitations. In this study, quercetin-based Pickering emulsions were synthesized and evaluated for their anticancer activity against hepatic cancer cells. Pickering emulsions are particularly attractive as nanocarriers owing to their biodegradability, minimal toxicity, facile synthesis, chemical modifiability, and biocompatibility (Andres *et al.*, 2018). Chitosan-tripolyphosphate (CS-TPP) nanoparticles were used as stabilizers to produce size-controlled Pickering emulsions with enhanced biological activity and improved stability.

Quercetin-loaded Pickering emulsions were prepared with minor modifications to previously reported protocols (Shah *et al.*, 2016). The emulsions remained stable at room temperature for at least 6 weeks (± 1.22), demonstrating greater stability as compared to several reported nanocarrier systems (ye *et al.*, 2021). Nanoparticles possess unique biological utility due to their high surface charge, which promotes interactions with natural compounds. In this formulation, nanoparticles served as stabilizers at the oil-water interface of the Pickering emulsion. Medium-chain triglycerides (MCTs), specifically lauric acid, were used as the oil phase. Within the body, lauric acid is either incorporated into newly synthesized triglycerides that enter the lymphatic system or, more commonly, transported directly to the liver. The structural properties of coconut-derived triglycerides facilitate more efficient digestion compared to other long-chain triglycerides, such as palmitic acid. Consequently, lauric acid exhibits a high clearance rate with minimal side effects, making it an effective component for targeted

drug delivery (Dayrit *et al.*, 2015). The CSNP-stabilized Pickering system developed in this study incorporates two major advantages that have been repeatedly identified in the recent literature: (1) the intrinsic interfacial robustness of particle-stabilized emulsions, and (2) the functional benefits of chitosan nanoparticles as stabilizers. Recent reviews highlight that PEs reduce the need for synthetic surfactants, improve physical stability against coalescence, and can enhance the biological accessibility of hydrophobic actives in nutraceutical and pharmaceutical contexts (Wang *et al.*, 2025). Recently, a study reported the synthesis of quercetin-loaded Pickering emulsions for tropical skin care applications in which chitosan nanoparticle was used as a solid stabilizer, which is in line with our study as well (Sainakham *et al.*, 2025).

The nanoparticles exhibited a smaller size than the synthesized Pickering emulsions due to interactions with oil and the encapsulated drug. The size distribution results were consistent with the previously reported study (Shah *et al.*, 2016). Controlled particle size is critical for efficient cellular uptake of CSNPs-QPE. UV-visible spectroscopy revealed absorption peaks at 378.8 nm and 341.9 nm for CSNPs-QPE and CSNPs-UPE, respectively. Quercetin alone displayed a characteristic peak at 375 nm, while nanoparticles exhibited a peak at 310 nm. The red shift from 375 to 378.8 nm indicates successful bonding between quercetin and the emulsion. FTIR analysis confirmed chemical interactions among emulsion components, with CSNPs-UPE showing characteristic absorption peaks at 2879, 2945, 916, 750, 1707, and 1286 cm^{-1} , whereas CSNPs-QPE exhibited a peak at 3304 cm^{-1} corresponding to phenolic OH of quercetin and surface hydroxyls and N-H stretching from chitosan (Fig. 3b). The 1448 cm^{-1} peak is attributed to aromatic C=C stretching / ring vibrations associated with phenolic

groups of quercetin and its appearance in CSNPs-QPE suggesting the presence of quercetin at the interface. A peak at 1230 cm⁻¹ is associated with C–O stretching / C–O–C vibrations (quercetin phenolic ether and lauric acid C–O) and phosphate-related vibrational modes from TPP–chitosan interactions (Fig. 3b). These data are consistent with previously reported findings (Kajbafvala et al., 2017), supporting the successful synthesis of the Pickering emulsions. A study conducted by Xu et al. also reported the broad absorption peak at 3400 cm⁻¹ along with a peak at 1500 cm⁻¹ depicting C–O stretching vibration (XU et al., 2019). FTIR results along with UV–visible spectra, suggesting multiple chemical modifications during emulsion formation.

Particle size distribution analysis revealed an average emulsion diameter of 238 nm with a surface charge of +59.5 mV. Nanoscale size (~238 nm) allows efficient internalization by cancer cells through endocytosis. Such emulsions can penetrate biological barriers more effectively, such as tumor interstitial spaces, and can improve drug deposition at the target site. Further +59.5 mV zeta potential demonstrates strong electrostatic repulsion among droplets to avoid agglomeration during storage or biological circulation. Another benefit of positive surface charge involves the electrostatic attraction to negatively charged phospholipid membranes of cancer cells, promoting better cellular adhesion and uptake of the encapsulated quercetin. The polydispersity index (PDI) of 0.457 (<1) indicates a uniform size distribution. The high zeta potential of the quercetin-loaded emulsions suggests strong electrostatic interactions between the oil and aqueous phases (Shah et al., 2016). Fluorescence imaging confirmed quercetin encapsulation, as quercetin is naturally fluorescent (Yang et al., 2017). Transmitted light images revealed spherical Pickering emulsion particles with smooth boundaries (Figs. 5a and b), consistent with dynamic light scattering (zeta sizer) measurements. Scanning electron microscopy (SEM) further confirmed the formation of uniformly shaped, size-controlled Pickering emulsions (Fig. 5c), in agreement with the findings of Albalawi et al. (Albalawi et al., 2023).

The Pickering emulsions achieved a high quercetin encapsulation efficiency of 88.8% (±0.95), exceeding values typically observed in comparable nano formulations (Rodríguez-Félix et al., 2019). High encapsulation efficiency enhances bioavailability and is often associated with smaller nanoparticle size (Rodríguez-Félix et al., 2019). The therapeutic efficacy of nanodrug systems depends on controlled drug release following administration. Sustained release offers several advantages, including reduced dosing frequency, fewer adverse effects, and prolonged therapeutic action (Albalawi et al., 2023). In this study, quercetin release from the Pickering emulsions followed a diffusion-controlled pattern, with higher release observed at pH 4.0 compared to pH 7.4. This pH-dependent behavior suggests preferential drug release in the acidic microenvironment of cancer cells (Abdella et al., 2023).

Cytotoxicity of the synthesized nanoformulation was assessed in HepG2 liver cancer cells. At a concentration of 80 µg/mL, CSNPs-QPE induced >90% cell death (Fig. 7a). At lower concentrations (5 µg/mL), both CSNPs-QPE and doxorubicin achieved approximately 50% cell inhibition (Fig. 7a). The half-maximal inhibitory concentration (IC₅₀) for CSNPs-QPE was 20 µg/mL after 48 hours of treatment, reflecting the time required for sustained drug release from the nanoformulation (Fig. 7b). MTT assay results demonstrated a dose-dependent decrease in cell viability, with the highest viability observed at 2.5 µg/mL and progressively reduced survival at higher concentrations. These findings are consistent with previous reports demonstrating effective inhibition of tumor cell proliferation following the administration of betanin-encapsulated nanoparticles to breast cancer cells (Rehman et al., 2023).

A wound-healing (scratch) assay was performed to evaluate the impact of CSNPs-QPE and doxorubicin on 2D tumor cell migration, a critical step in metastasis involving cell movement through the extracellular matrix. The wound-healing assay revealed that CSNPs-QPE significantly suppressed the lateral migration of HepG2 cells in a two-dimensional environment, indicating strong inhibition of a key early step in tumor metastasis. Both tested concentrations (5 and 20 µg/mL) produced markedly greater inhibition of scratch closure compared with doxorubicin, underscoring the enhanced antimetastatic potential of the Pickering emulsion system. These results align with earlier reports that nanoparticle-based CuS@mSiO₂-PEG formulations impede

cancer cell motility by disrupting cytoskeletal remodeling and adhesion signaling (Deng et al., 2018).

Recent research studies highlight the effective delivery of macromolecules by nanoparticles targeting multiple proteins involved in tumor progression (Dong et al., 2023; Das et al., 2024; Kapoor et al., 2025). Aberrant activation of the PI3K/Akt/mTOR signaling pathway is a key driver of hepatocellular carcinoma, promoting uncontrolled proliferation, angiogenesis, and metastasis while also contributing to chemoresistance (Sorice et al., 2014; Dong et al., 2021). The present study demonstrates that quercetin-loaded chitosan Pickering emulsions (CSNPs-QPE) markedly downregulate the PI3K/Akt/mTOR signaling cascade in HepG2 cells, with more than 80% inhibition of PI3K and mTOR gene expression (Figs. 9 and 13) and significant suppression of Akt and mTOR even at low concentrations (5 µg/mL) (Figs. 11c and 13c) indicating potent antiproliferative effects. These results are consistent with earlier reports showing that quercetin can modulate PI3K/Akt/mTOR signaling to inhibit hepatocellular carcinoma (HCC) progression (Dong et al., 2021). Another study illustrated the antitumor activity of quercetin nanoparticles by inactivating the protein expression level of Akt and ERK1/2 signaling pathway in liver cancer cells (Zhang et al., 2025). Compared with these carriers, the CSNPs-QPE developed in this study achieved lower IC₅₀ values for PI3K, Akt, and mTOR inhibition than doxorubicin, indicating enhanced potency (Figs. 10, 12, and 14). In Fig. 10, lower IC₅₀ values of CSNPs-QPE (4.5 µg/mL) for inhibiting PI3K expression in comparison to doxorubicin (6.67 µg/mL) illustrate its greater potency. The same observations were recruited from analysis of IC₅₀ values of CSNPs-QPE for inhibiting Akt and mTOR expression pattern (Figs. 12 and 14). Particularly, IC₅₀ values of CSNPs-QPE (2.244 µg/mL) for inhibiting mTOR depicted more therapeutic potency in comparison to doxorubicin (10.01 µg/mL) (Fig. 14). This therapeutic effectivity may be attributed to the unique interfacial stabilization and high surface charge of Pickering emulsions, which can improve cellular uptake and sustained drug release relative to conventional liposomes or polymeric nanoparticles. Furthermore, the ability of CSNPs-QPE to significantly suppress mTOR expression at lower doses signifies their potential to overcome mTOR-driven chemoresistance, a major limitation of current HCC therapies. Quercetin primarily exerts its anticancer effects in HCC by downregulating P4HA2 and promoting Phosphatase and Tensin Homolog (PTEN) activation, thereby inhibiting the PI3K/Akt/mTOR signaling pathway. This mechanism positions quercetin as a promising therapeutic strategy against HCC (Zhang et al., 2025; Karabat et al., 2025). Based on these previous studies, we coupled the therapeutic efficacy of quercetin by incorporating it into Pickering emulsions to improve cellular uptake, increased intracellular retention and sustained release of drug. Taken together, these findings extend previous evidence on quercetin nanoformulations by demonstrating that chitosan-based Pickering emulsions offer an effective and biocompatible platform for targeted regulation of the PI3K/Akt/mTOR pathway.

5. Conclusions

Biodegradable quercetin-encapsulated chitosan Pickering emulsions exhibited significant *in vitro* cytotoxicity against human liver cancer cells, accompanied by inhibition of cell migration and downregulation of the PI3K/Akt/mTOR signaling pathway. The emulsions also demonstrated sustained quercetin release, indicating their potential as a controlled nano-drug delivery system. While these findings highlight CSNPs-QPE as a promising platform for quercetin delivery, the evidence is currently limited to *in vitro* experiments. Comprehensive preclinical studies and scale up evaluations are essential before any clinical translation.

CRedit authorship contribution statement

Zainab Noreen: Investigation, data curation, writing – original draft. **Mariam Naveed:** Investigation, data curation, writing – original draft. **Abida Raza Rao:** Investigation, resources. **Shahid Masood Shah:** Investigation, resources. **Bushra Ijaz:** Investigation, resources. **Imran**

Shahid: Formal analysis, statistical analysis. **Abdullah R. Alzahrani:** Formal analysis, statistical analysis. **Sidra Rehman:** Conceptualization, supervision, writing – review and editing.

Declaration of competing interest

The authors declare that they have no competing financial interests or personal relationships that could have influenced the work presented in this paper..

Data availability

The authors confirm that the data supporting the findings of this study are available within the article.

Declaration of Generative AI and AI-assisted technologies in the writing process

The authors confirm that there was no use of Artificial Intelligence (AI)-Assisted Technology for assisting in the writing or editing of the manuscript and no images were manipulated using AI.

Acknowledgement

The authors extend their appreciation to Umm Al-Qura University, Saudi Arabia for funding this research work through grant number: 25UQU4330924GSSR05

Funding statement

This research work was funded by Umm Al-Qura University, Saudi Arabia under grant number: 25UQU4330924GSSR05

References

- Abdella, S., Abid, F., Youssef, S.H., Kim, S., Afinuomu, F., Malinga, C., Song, Y., Garg, S., 2023. pH and its applications in targeted drug delivery. *Drug Discov Today* 28, 103414. <https://doi.org/10.1016/j.drudis.2022.103414>
- Albalawi, F., Hussein, M.Z., Fakurazi, S., Masarudin, M.J., 2023. Fabrication and characterization of nanodelivery platform based on chitosan to improve the anticancer outcome of sorafenib in hepatocellular carcinoma. *Sci Rep* 13, 12180. <https://doi.org/10.1038/s41598-023-38054-4>
- Andres, S., Pevny, S., Ziegenhagen, R., Bakhiya, N., Schäfer, B., Hirsch-Ernst, K.I., Lampen, A., 2018. Safety aspects of the use of quercetin as a dietary supplement. *Mol Nutr Food Res* 62. <https://doi.org/10.1002/mnfr.201700447>
- Aranaz, I., Alcántara, A.R., Civera, M.C., Arias, C., Elorza, B., Heras Caballero, A., Acosta, N., 2021. Chitosan: An overview of its properties and applications. *Polymers (Basel)* 13, 3256. <https://doi.org/10.3390/polym13193256>
- Bahuguna, A., Khan, I., Bajpai, V.K., Kang, S.C., 2017. MTT assay to evaluate the cytotoxic potential of a drug. *Bangladesh J Pharmacol* 12. <https://doi.org/10.3329/bjpp.v12i2.30892>
- Bayat Mokhtari, R., Homayouni, T.S., Baluch, N., Morgatskaya, E., Kumar, S., Das, B., Yeger, H., 2017. Combination therapy in combating cancer. *Oncotarget* 8, 38022-38043. <https://doi.org/10.18632/oncotarget.16723>
- Ben-Arye, E., Schiff, E., Hassan, E., Mutafoğlu, K., Lev-Ari, S., Steiner, M., Lavie, O., Polliack, A., Silbermann, M., Lev, E., 2012. Integrative oncology in the middle East: From traditional herbal knowledge to contemporary cancer care. *Ann Oncol* 23, 211-221. <https://doi.org/10.1093/annonc/mdr054>
- Bray, F., Laversanne, M., Weiderpass, E., Soerjomataram, I., 2021. The ever-increasing importance of cancer as a leading cause of premature death worldwide. *Cancer* 127, 3029-3030. <https://doi.org/10.1002/cncr.33587>
- Chen, H., Feng, X., Gao, L., Mickymaray, S., Paramasivam, A., Abdulaziz Alfaiz, F., Almasmoum, H.A., Ghaith, M.M., Almamaini, R.A., Aziz Ibrahim, I.A., 2021. Inhibiting the PI3K/AKT/mTOR signalling pathway with copper oxide nanoparticles from *Houttuynia cordata* plant: Attenuating the proliferation of cervical cancer cells. *Artif Cells Nanomed Biotechnol* 49, 240-249. <https://doi.org/10.1080/21691401.2021.1890101>
- Chen, Y., Liu, Y., Liu, H., Gao, Y., 2021. Preparation of lauric acid modified high-amylose cornstarch by a solvothermal process and its pickering emulsion. *ACS Food Sci Technol* 1, 845-853. <https://doi.org/10.1021/acfoodsctech.1c00058>
- Das, U., Kapoor, D.U., Singh, S., Prajapati, B.G., 2024. Unveiling the potential of chitosan-coated lipid nanoparticles in drug delivery for management of critical illness: A review. *Z Naturforsch C J Biosci* 79, 107-124. <https://doi.org/10.1515/znc-2023-0181>
- Dayrit, F.M., 2015. The properties of lauric acid and their significance in coconut oil. *J Americ Oil Chem Soc* 92, 1-15. <https://doi.org/10.1007/s11746-014-2562-7>
- Dehelean, C.A., Marcovici, I., Soica, C., Mioc, M., Coricovac, D., Iurciuc, S., Cretu, O.M., Pinzaru, I., 2021. Plant-derived anticancer compounds as new perspectives in drug discovery and alternative therapy. *Molecules* 26, 1109. <https://doi.org/10.3390/molecules26041109>
- Deng, G., Zhou, F., Wu, Z., Zhang, F., Niu, K., Kang, Y., Liu, X., Wang, Q., Wang, Y., Wang, Q., 2017. Inhibition of cancer cell migration with CuS@mSiO₂-PEG nanoparticles by repressing MMP-2/MMP-9 expression. *Int J Nanomedicine* 13, 103-116. <https://doi.org/10.2147/IJN.S148487>
- Dong, C., Wu, J., Chen, Y., Nie, J., Chen, C., 2021. Activation of PI3K/AKT/mTOR pathway causes drug resistance in breast cancer. *Front Pharmacol* 12, 628690. <https://doi.org/10.3389/fphar.2021.628690>
- Dong, L., Ding, J., Zhu, L., Liu, Y., Gao, X., Zhou, W., 2023. Copper carbonate nanoparticles as an effective biomimetic carrier to load macromolecular drugs for multimodal therapy. *Chin Chem Lett* 34, 108192. <https://doi.org/10.1016/j.ccllet.2023.108192>
- Furuta, Y., Manita, D., Hirowatari, Y., Shoji, K., Ogata, H., Tanaka, A., Kawabata, T., 2023. Postprandial fatty acid metabolism with coconut oil in young females: A randomized, single-blind, crossover trial. *Am J Clin Nutr* 117, 1240-1247. <https://doi.org/10.1016/j.ajcnut.2023.03.015>
- Gersten, O., Wilmoth, J.R., 2002. The cancer transition in Japan since 1951. *DemRes* 7, 271-306. <https://doi.org/10.4054/demres.2002.7.5>
- Guruvayoorappan, C., Sakthivel, K.M., Padmavathi, G., Bakliwal, V., Monisha, J., Kunnumakkara, A.B., 2015. Cancer preventive and therapeutic properties of fruits and vegetables: An overview. *Anticancer properties of fruits and vegetables: A scientific review*. 2015, 1-52. https://doi.org/10.1142/9789814508896_0001
- Hashemzaei, M., Delarami Far, A., Yari, A., Heravi, R.E., Tabrizian, K., Taghdisi, S.M., Sadeh, S.E., Tsarouhas, K., Kouretas, D., Tzanakakis, G., Nikitovic, D., Anisimov, N.Y., Spandidos, D.A., Tsatsakis, A.M., Rezaee, R., 2017. Anticancer and apoptosis-inducing effects of quercetin in vitro and in vivo. *Oncol Rep* 38, 819-828. <https://doi.org/10.3892/or.2017.5766>
- Islam, N.U., Amin, R., Shahid, M., Amin, M., Zaib, S., Iqbal, J., 2017. A multi-target therapeutic potential of *Prunus domestica* gum stabilized nanoparticles exhibited prospective anticancer, antibacterial, urease-inhibition, anti-inflammatory and analgesic properties. *BMC Complement Altern Med* 17, 276. <https://doi.org/10.1186/s12906-017-1791-3>
- Jamil, B., Abbasi, R., Abbasi, S., Imran, M., Khan, S.U., Ihsan, A., Javed, S., Bokhari, H., Imran, M., 2016. Encapsulation of cardamom essential oil in chitosan nano-composites: *In-vitro* efficacy on antibiotic-resistant bacterial pathogens and cytotoxicity studies. *Front Microbiol* 7, 1580. <https://doi.org/10.3389/fmicb.2016.01580>
- Jiang, J., Zheng, Q., Yan, Y., Guo, D., Wang, F., Wu, S., Sun, W., 2018. Design of a novel nanocomposite with C-s-h@LA for thermal energy storage: A theoretical and experimental study. *Appl Energy* 220, 395-407. <https://doi.org/10.1016/j.apenergy.2018.03.134>
- Kajbafvala, A., Salabat, A., 2017. A novel one-step microemulsion method for preparation of quercetin encapsulated poly(methyl methacrylate) nanoparticles. *Iran Polym J* 26, 651-662. <https://doi.org/10.1007/s13726-017-0550-0>
- Kapoor, D.U., Pareek, A., Patel, S., Fareed, M., Alsaïdan, O.A., Prajapati, B.G., 2025. Advances in cancer therapy using fluorinated chitosan: A promising nanoplatform for drug delivery. *Med Oncol* 42, 452. <https://doi.org/10.1007/s12032-025-03022-7>
- Karabat, M.U., Tuncer, M.C., 2025. PI3K/Akt1 Pathway suppression by quercetin-doxorubicin combination in osteosarcoma cell line (MG-63 Cells). *Medicina* 61, 1347. <https://doi.org/10.3390/medicina61081347>
- Kyriakides, T.R., Raj, A., Tseng, T.H., Xiao, H., Nguyen, R., Mohammed, F.S., Halder, S., Xu, M., Wu, M.J., Bao, S., Sheu, W.C., 2021. Biocompatibility of nanomaterials and their immunological properties. *Biomed Mater* 16, 1748-605X. <https://doi.org/10.1088/1748-605X/abe5fa>
- Lima Cardial, M.R., Paula, H.C.B., da Silva, R.B.C., da Silva Barros, J.F., Richter, A.R., Sombra, F.M., de Paula, R.C.M., 2019. Pickering emulsions stabilized with cashew gum nanoparticles as indomethacin carrier. *Int J Biol Macromol* 132, 534-540. <https://doi.org/10.1016/j.ijbiomac.2019.03.198>
- Rehman, Z., Naveed, M., Ijaz, B., Musaddiq Shah, M., Shahid, I., Tarique Imam, M., Saeed Al Malki, Z., Rehman, S., 2023. Evaluation of betanin-encapsulated biopolymeric nanoparticles for antitumor activity via PI3K/Akt/mTOR signaling pathway. *Arab J Chem* 16, 105323. <https://doi.org/10.1016/j.arabjc.2023.105323>
- Rodríguez-Félix, F., Del-Toro-Sánchez, C.L., Javier Cinco-Moroyoqui, F., Juárez, J., Ruiz-Cruz, S., López-Ahumada, G.A., Carvajal-Millan, E., Castro-Enríquez, D.D., Barreras-Urbina, C.G., Tapia-Hernández, J.A., 2019. Preparation and characterization of quercetin-loaded zein nanoparticles by electrospinning and study of *In Vitro* Bioavailability. *J Food Sci* 84, 2883-2897. <https://doi.org/10.1111/1750-3841.14803>
- Sainakhm, M., Arunlakvilart, P., Samran, N., Vivattanaseth, P., Preedalikit, W., 2025. Formulation and stability of quercetin-loaded pickering emulsions using chitosan/gum arabic nanoparticles for topical skincare applications. *Polymers (Basel)* 17, 1871. <https://doi.org/10.3390/polym17131871>
- Shah, B.R., Li, Y., Jin, W., An, Y., He, L., Li, Z., Xu, W., Li, B., 2016. Preparation and optimization of Pickering emulsion stabilized by chitosan-tripolyphosphate nanoparticles for curcumin encapsulation. *Food Hydrocoll* 52, 369-377. <https://doi.org/10.1016/j.foodhyd.2015.07.015>
- Sorice, A., Guerriero, E., Capone, F., Colonna, G., Castello, G., Costantini, S., 2014. Ascorbic acid: Its role in immune system and chronic inflammation diseases. *Mini Rev Med Chem* 14, 444-452. <https://doi.org/10.2174/1389557514666140428112602>
- Sung, H., Ferlay, J., Siegel, R.L., Laversanne, M., Soerjomataram, I., Jemal, A., Bray, F., 2021. Global cancer statistics 2020: GLOBOCAN estimates of incidence and

- mortality worldwide for 36 cancers in 185 countries. *CA Cancer J Clin* 71, 209-249. <https://doi.org/10.3322/caac.21660>
- Vafadar, A., Shabaninejad, Z., Movahedpour, A., Fallahi, F., Taghavipour, M., Ghasemi, Y., Akbari, M., Shafiee, A., Hajighadimi, S., Moradizarmehri, S., Razi, E., Savardashtaki, A., Mirzaei, H., 2020. Quercetin and cancer: New insights into its therapeutic effects on ovarian cancer cells. *Cell Biosci* 10, 32. <https://doi.org/10.1186/s13578-020-00397-0>
- Virmani, T., Kumar, G., Sharma, A., Pathak, K., Akhtar, M.S., Afzal, O., Altamimi, A.S.A., 2023. Amelioration of cancer employing chitosan, its derivatives, and chitosan-based nanoparticles: recent updates. *Polymers (Basel)* 15, 2928. <https://doi.org/10.3390/polym15132928>
- Wang, S., Lin, J., Wang, Z., Zhou, Z., Bai, R., Lu, N., Liu, Y., Fu, X., Jacobson, O., Fan, W., Qu, J., Chen, S., Wang, T., Huang, P., Chen, X., 2017. Core-satellite polydopamine-gadolinium-metallofullerene nanotheranostics for multimodal imaging guided combination cancer therapy. *Adv Mater* 29. <https://doi.org/10.1002/adma.201701013>
- Wang, W., Sun, C., Mao, L., Ma, P., Liu, F., Yang, J., Gao, Y., 2016. The biological activities, chemical stability, metabolism and delivery systems of quercetin: A review. *Trends Food Sci & Technol* 56, 21-38. <https://doi.org/10.1016/j.tifs.2016.07.004>
- Wang, X., Tian, N., He, L., Yuan, Z., Han, L., 2025. Emerging applications of pickering emulsions in pharmaceutical formulations: A comprehensive review. *Int J Nanomedicine* 20, 5923-5947. <https://doi.org/10.2147/IJN.S514928>
- Xu, T., Gao, C., Feng, X., Yang, Y., Shen, X., Tang, X., 2019. Structure, physical and antioxidant properties of chitosan-gum Arabic edible films incorporated with cinnamon essential oil. *Int J Biol Macromol* 134, 230-236. <https://doi.org/10.1016/j.ijbiomac.2019.04.189>
- Yang, Y., Fang, Z., Chen, X., Zhang, W., Xie, Y., Chen, Y., Liu, Z., Yuan, W., 2017. An overview of pickering emulsions: Solid-particle materials, classification, morphology, and applications. *Front Pharmacol* 8, 287. <https://doi.org/10.3389/fphar.2017.00287>
- Ye, J., Li, R., Yang, Y., Dong, W., Wang, Y., Wang, H., Sun, T., Li, L., Shen, Q., Qin, C., Xu, X., Liao, H., Jin, Y., Xia, X., Liu, Y., 2021. Comparative colloidal stability, antitumor efficacy, and immunosuppressive effect of commercial paclitaxel nanoformulations. *J Nanobiotechnology* 19, 199. <https://doi.org/10.1186/s12951-021-00946-w>
- Zhang, J., Guo, J., Qian, Y., Yu, L., Ma, J., Gu, B., Tang, W., Li, Y., Li, H., Wu, W., 2025. Quercetin Induces Apoptosis Through Downregulating P4HA2 and Inhibiting the PI3K/Akt/mTOR Axis in Hepatocellular Carcinoma Cells: An In Vitro Study. *Cancer Rep (Hoboken)* 8, e70220. <https://doi.org/10.1002/cnr.2.70220>